Cambridge Centre for Computational Chemical Engineering

University of Cambridge

Department of Chemical Engineering

Preprint ISSN 1473 – 4273

Modelling and validation of granulation with heterogeneous binder dispersion and chemical reaction

Andreas Braumann [1] , Mike J. Goodson [1] , Markus Kraft [1] ,

Paul R. Mort [2]

released: 30 May 2006

[1] Department of Chemical Engineering
University of Cambridge
Pembroke Street
Cambridge CB2 3RA
UK
E-mail: mk306@cam.ac.uk

[2] Procter and Gamble Co.
ITC
5299 Spring Grove Avenue
Cincinnati, OH 45217
USA

Preprint No. 40

c4e

Key words and phrases: granulation, agglomeration, product design, particle formation, dispersion, reactive binder

Edited by
Cambridge Centre for Computational Chemical Engineering
Department of Chemical Engineering
University of Cambridge
Cambridge CB2 3RA
United Kingdom.

Fax: + 44 (0)1223 334796
E-Mail: c4e@cheng.cam.ac.uk
World Wide Web: http://www.cheng.cam.ac.uk/c4e/

Abstract

In this paper a multidimensional model for binder granulation is presented. The particles undergo different transformations such as coalescence, compaction, and breakage. Further chemical reaction in the granules is taken into account in order to incorporate binder solidification which is observed to be a significant transformation in many industrial applications. The equations of the model framework are solved numerically with a direct simulation Monte Carlo (DSMC) algorithm. In addition to the comparison between experiment and simulation, the model framework also enables the study of critical parameters in binder granulation such as reaction rate (solidification of binder) and size of the added binder droplets, which demonstrates its promising potential.

Contents

1 Introduction and background **5**

2 Details of the model **6**

2.1 Particle description 6

2.2 Transformations and their rules 7

2.2.1 Addition of binder 8

2.2.2 Coalescence of particles 8

2.2.3 Compaction 10

2.2.4 Chemical reaction 10

2.2.5 Penetration 11

2.2.6 Breakage 12

2.3 Numerical solution 13

3 Discussion of simulation results and experimental validation **13**

3.1 Comparison between experiment and simulation 14

3.2 Parameter variations 18

4 Conclusions **20**

1 Introduction and background

Granulation is a common industrial process which transforms fine powders into coarser grains that are user-friendly for handling, storage, post-processing, re-dispersion, and other processing or usage needs. Benefits include improved flowability and compaction behaviour for subsequent industrial processes (pharmaceutical tabletting, ceramic dry forming, minerals processing), storage stability, handling and re-dispersion required by end-use applications (foods, detergents, agricultural chemicals, etc.). Besides the improvement to powder handling, granulation is also used to create ordered micro-mixtures of different components [18], to prevent segregation and to control dissolution [11, 27].

Granulation is often accomplished using a liquid binder to create a composite structure of fine particles connected by a binder phase. In the granular product, the binder is usually converted into a stable solid phase, for example by drying, cooling or reaction of the binder with the particulate substrate. The conversion of the binder from a liquid to a solid state can be done as a post-process (e.g., a separate drying step) or it can be an integral part of the granulation process. In the latter case, the rate of the binder transformation from liquid to solid is critical to the granulation process.

Binder granulation is typically achieved by adding a liquid binder to small solid particles in a mixer-granulator, fluidised bed or other appropriate unit operation. The binder can be atomized as individual droplets contacting the particle bed [8] or as a liquid stream that is dispersed by contact transfer in a mechanically-induced shear field. Alternatively, a binder can be added as a solid particulate, and then brought to a liquid or soft-solid state during the granulation process, as in hot melt [22]. Flow and shear fields within the process induce collisions between particles and further the dispersion and transfer of the binder [23]. The stress associated with these collisions and the dissipation of energy by viscous binder layers and/or plastic deformation of the granular structures is fundamental to the mechanics of the granulation process. While the particles are bound due to capillary pressure, surface tension and viscous forces related to the binder phase [9], the critical properties of the binder itself are often changing during the process. On the one hand, the transformation of the binder can be advantageous for process control; on the other, it adds additional complexity to a system that is already undergoing multiple concurrent transformations. Similarly, breakage may be desired to limit the growth of the granules [25], so that the product is more homogeneous in size [20] and composition [26], but the stochastic nature of breakage adds a lot of complexity to the modelling and processing.

Previous work suggests an approach to analyse and optimise binder granulation processes in terms of micro-scale transformations [16]. It is suggested to first identify the critical transformations relating to a specific product specification and/or process operation; then, wherever possible, to strategically separate these transformations in order to optimise the control of the process. Further, a practical example of process optimisation and control by the spatial and/or temporal separation of critical transformations has been documented [17].

In the current work, the authors aim to further the scientific approach to granulation product optimisation and process control through a stochastic modelling framework. This modelling framework provides a multivariate population balance capable of concurrent

transformations while tracking multiple product attributes. The output of the model is a set of predictive process trajectories for distributed product attributes including size, granule density and composition. While the modelling work is still at a research stage, the mathematical algorithms are of reasonable efficiency for application to process optimisation and control.

The stochastic modelling framework permits the use of both continuous descriptions (based on empirical approximations applied to the bulk system) and discrete events (based on micro-scale models). Relevant transformations include binder atomization, binder dispersion, nucleation, granule coalescence, layering, compaction, binder solidification (e.g., by reaction, drying, cooling), and breakage (fragmentation, abrasion). Significantly, the description of transformations as discrete events on a micro-scale allows the direct incorporation of mechanistic models in the overall process model framework. As such, the stochastic method enables a significant bridging of scales from first-principle micro-scale to the process unit operation.

A significant outcome of the current work is the incorporation of an explicit binder transformation rate within the granulation process. In practice, binder transformation (e.g., from a liquid to solid phase) is observed in reactive binder systems (reaction rate), agglomeration with concurrent drying (drying rate) and hot melt granulation (cooling rate). In all cases, the relevant rate processes occur on a per granule basis, as a function of the granule composition and process history. Whereas previous empirical models may approximate the effect of such transformations on a bulk scale, the current modelling framework allows the use of detailed mechanistic models on a micro-scale using fundamental physical and chemical properties.

Overall, the potential to bridge the micro (i.e., granule) and unit-operation scales using the stochastic modelling approach is a very promising development. Enabling the use of first-principle models as elements in an overall process description can help to supplant the empiricism that pervades much of the current practice in particulate processes [2], with the potential to both improve process efficiency and product quality.

2 Details of the model

2.1 Particle description

Historically, particle size has been used as the primary attribute in population balance models [13, 21, 1]. The current work takes a more comprehensive perspective, tracking compositional and structural features of the granules, giving rise to the size, porosity and compositional distributions of the granules.

In general, the current model tracks the volume of solid, liquid and vapour phases in a representative sampling of individual granules. The solid volume includes the particulate volume associated with constituent particles (original solid) along with any solid reaction products of binders (reacted solid). Liquid binder is partitioned by location, either on the surface of particles or internal to the granule structure. In the latter case, the internal binder occupies granular pore volume. The remaining pore volume is filled with a vapour

Table 1: *Variables describing a granule*

dependency	variable	notation
independent	original solid volume	s_o
	reacted solid volume	s_r
	external liquid volume	l_e
	internal liquid volume	l_i
	pore volume	p
dependent	total volume	v
	external surface area	a_e
	internal surface area	a_i
	porosity	ε

phase. The shape of a granule is assumed to be spherical. In total, a granule is described by five independent variables. From these it is possible to express other properties such as the total volume (particle size) or the surface area. Table 1 summarises the variables that describe a particle.

The vector x of independent variables which describe a granule therefore has the form:

$$x = (s_\mathrm{o}, s_\mathrm{r}, l_\mathrm{e}, l_\mathrm{i}, p) \tag{1}$$

and is an element of the type space E. There exists relationships between the different variables, which are summarised in the following equations. The total granule volume v is obtained by

$$v = s_\mathrm{o} + s_\mathrm{r} + l_\mathrm{e} + p. \tag{2}$$

As the particle is a sphere, the external surface area a_e can be derived from the total volume v,

$$a_\mathrm{e} = \pi^{1/3} \, (6\, v)^{2/3}. \tag{3}$$

The internal surface area is considered to be proportional to the pore volume,

$$a_\mathrm{i} = \mathrm{C}\, p^{2/3} \qquad \text{with} \quad \mathrm{C} \geq \pi^{1/3}\, 6^{2/3} \approx 4.836, \tag{4}$$

and the porosity ε becomes

$$\varepsilon = \frac{p}{v}. \tag{5}$$

2.2 Transformations and their rules

The granular ensemble changes during the granulation process due to transformations taking place, i. e. events and mechanisms. We consider following transformations to take place in the current model:

1. Addition of binder
2. Coalescence of particles
3. Compaction (porosity reduction)
4. Chemical reaction
5. Mass transfer of liquid into the pores (penetration)
6. Breakage

2.2.1 Addition of binder

In the present case we consider the binder liquid to be added into the process by an implied process of droplet formation followed by contacting the solid particles with the liquid droplets. Together, the particles and droplets are the constituents of the granular ensemble. For the purpose of modelling, the droplets are represented as a special case of a particle; the vector of the independent variables for a droplet becomes

$$x_{\text{droplet}} = (0, 0, l_{\text{e}}, 0, 0). \tag{6}$$

The addition of binder is determined by the liquid flowrate and the droplet size distribution. For example, in a practical application using binder atomization, the droplet population depends on the nozzle configuration and operating parameters. In addition, the model allows for further droplet breakup and contact spreading in the process shear field, as described in the breakage section.

2.2.2 Coalescence of particles

For the further modelling it is assumed that the particle system of our granulation process is ideally mixed. The coagulation kernel $K(x, x')$, which gives the rate for the coalescence of particles with properties x and x' respectively, can be split into two parts

$$K(x, x') = K_0 \, \widetilde{K}(x, x'). \tag{7}$$

The term K_0 is independent of the properties of the two colliding particles and lumps the general conditions of the flow field in the process. It is also referred to as collision rate. The term $\widetilde{K}$ accounts for the probability of a successful coalescence and becomes either 1 (coalescence) or 0 (no coalescence). The physically based STOKES criterion [4] is used to decide whether or not two particles coalesce. According to this criterion, a collision leads to coalescence if the kinetic energy of the two colliding particles is dissipated in the viscous binder layer. The solution of the momentum balance [4] leads to the viscous STOKES number St_{v}:

$$\mathrm{St}_{\text{v}} = \frac{\text{collision energy}}{\text{energy of viscous dissipation}} = \frac{\widetilde{m}\, U}{3\,\pi\,\eta\,\widetilde{R}^{\,2}}, \tag{8}$$

where $\widetilde{m}$ is the harmonic mean granule mass, U is the collision velocity, η is the binder viscosity, and $\widetilde{R}$ is the harmonic mean particle radius.

Coalescence takes place if the critical STOKES number St_v^* is bigger than the viscous STOKES number St_v.

$$\begin{aligned} \mathrm{St}_\mathrm{v} \leq \mathrm{St}_\mathrm{v}^* &: \widetilde{K} = 1 : \text{coalescence} \\ \mathrm{St}_\mathrm{v} > \mathrm{St}_\mathrm{v}^* &: \widetilde{K} = 0 : \text{no coalescence.} \end{aligned} \tag{9}$$

The critical STOKES number St_v^* is defined by:

$$\mathrm{St}_\mathrm{v}^* = \left(1 + \frac{1}{e_\mathrm{coag}}\right) \ln\left(\frac{h}{h_\mathrm{a}}\right), \tag{10}$$

where e_coag is the coefficient of restitution, h is the thickness of the binder layer, and h_a is the characteristic length scale of surface asperities. The coefficient of restitution in eq. (10) is defined as the geometric average of the coefficients of restitution of the single particles (j, k),

$$e_\mathrm{coag} = \sqrt{e_j \cdot e_k}. \tag{11}$$

A mass-weighted arithmetic average is used for the calculation of the coefficient of restitution e_j of each particle core,

$$e_j = \frac{\sum\limits_{\alpha \in \{s_\mathrm{o}, s_\mathrm{r}, l_\mathrm{i}\}} e_\alpha \, m_\alpha}{\sum\limits_{\alpha \in \{s_\mathrm{o}, s_\mathrm{r}, l_\mathrm{i}\}} m_\alpha}. \tag{12}$$

The coefficient of restitution e is the ratio of rebound energy to impact energy, and hence it takes values between zero (totally plastic impact) and one (totally elastic impact). We assume that the coefficient of restitution e for liquid is zero.

If the two particles (j, k) coalesce, the properties of the new particle are calculated as follows:

$$s_\mathrm{o} = s_{\mathrm{o},j} + s_{\mathrm{o},k}, \tag{13}$$

$$s_\mathrm{r} = s_{\mathrm{r},j} + s_{\mathrm{r},k}, \tag{14}$$

$$l_\mathrm{e} = l_{\mathrm{e},j} + l_{\mathrm{e},k} - l_{\mathrm{e}\to\mathrm{i}}, \tag{15}$$

$$l_\mathrm{i} = l_{\mathrm{i},j} + l_{\mathrm{i},k} + l_{\mathrm{e}\to\mathrm{i}}. \tag{16}$$

In equations (15) and (16) it is taken into account that a certain amount of external liquid becomes internal liquid due to the coagulation. This volume is computed by

$$l_{\mathrm{e}\to\mathrm{i}} = \frac{l_{\mathrm{e},j} + l_{\mathrm{e},k}}{2} \left[1 - \sqrt{1 - \left(\frac{\sqrt[6]{(v_j - l_{\mathrm{e},j}) \cdot (v_k - l_{\mathrm{e},k})}}{\sqrt[3]{v_j} + \sqrt[3]{v_k}}\right)^2}\right]. \tag{17}$$

This formulation satisfies that the converted volume $l_{\mathrm{e}\to\mathrm{i}}$ is low for $v_j - l_{\mathrm{e},j} \to 0$ and for the other particle respectively. Finally the pore volume of the new granules has to be

defined. Therefore, we follow an approach from [7], where it is proposed that the external surface area and the pore volume of the new granule depend on the softness of the two former particles. The coefficient of restitution e_{coag}, which is a measure of the softness of the particles, is used for the calculation of the external surface area of the new formed granule:

$$a_{\mathrm{e}} = (1 - e_{\mathrm{coag}}) \left(a_{\mathrm{e},j}^{3/2} + a_{\mathrm{e},k}^{3/2} \right)^{2/3} + e_{\mathrm{coag}} \left(a_{\mathrm{e},j} + a_{\mathrm{e},k} \right), \tag{18}$$

so that the pore volume of the newly formed particle becomes

$$p = \frac{a_{\mathrm{e}}^{3/2}}{6\sqrt{\pi}} - s_{\mathrm{o}} - s_{\mathrm{r}} - l_{\mathrm{e}}. \tag{19}$$

2.2.3 Compaction

Each collision of particles leads to compaction and will be described by an adapted approach using the findings of [10]. This means compaction is considered to be a subevent of coalescence and shall happen in the current model irrespective of whether coalescence is successful or not. The approach in [10] uses an empirical model which predicts the average porosity of a particle ensemble. For the time being, it is assumed that this approach can be followed for single granules too, so that the porosity change $\Delta\varepsilon$ due to collision is described by:

$$\Delta\varepsilon = \begin{cases} k_{\mathrm{porred}}\, U\, (\varepsilon - \varepsilon_{\mathrm{min}}) & \text{, if} \quad \varepsilon - \Delta\varepsilon \geq \varepsilon_{\mathrm{min}} \\ 0 & \text{, otherwise,} \end{cases} \tag{20}$$

where k_{porred} is the rate constant of porosity reduction, U is the collision velocity, and $\varepsilon_{\mathrm{min}}$ is the minimum porosity.

In the current model, compaction causes transfer of internal liquid to the external surface once the pores are totally saturated by internal liquid.

2.2.4 Chemical reaction

Chemical interactions between the different components of the granules have to be taken into account for many applications in industrial practice. For example, hydration of substrate powders by aqueous binder systems and acid-base reactions are well known in industry. Variations in the chemical and physical characteristics of the raw materials can have a significant effect on the process. So far, this transformation has not been incorporated explicitly into a general process model framework.

For the present case we consider the formation of reacted solid from liquid binder, i. e. the solidification of the material. This continuous process happens when original solid material is present. It is assumed that the incremental conversion is proportional to the reaction interface, i. e. the surface area. Additionally, the reaction rate may be limited by transport across a product layer [12]. These considerations lead to the following equations for the reaction rates r_{reac}:

Reaction on the external surface:

$$r_{\mathrm{reac,e}} = \begin{cases} k_{\mathrm{reac,e}}\, a_{\mathrm{e}}\, \dfrac{l_{\mathrm{e}}}{l_{\mathrm{e}} + s_{\mathrm{r}}} & \text{, if} \quad s_o > 0 \text{ and } l_{\mathrm{e}} > 0 \\ 0 & \text{, otherwise.} \end{cases} \tag{21}$$

Reaction on the internal surface:

$$r_{\mathrm{reac,i}} = \begin{cases} k_{\mathrm{reac,i}}\, a_{\mathrm{i}}\, \dfrac{l_{\mathrm{i}}}{l_{\mathrm{i}} + s_{\mathrm{r}}} & \text{, if} \quad s_o > 0 \text{ and } l_{\mathrm{i}} > 0 \\ 0 & \text{, otherwise.} \end{cases} \tag{22}$$

Due to the reactions the particles become harder as the coefficient of restitution changes. The amount of external liquid will be reduced so that coalescence is less likely. Furthermore, the conversion of internal liquid into reacted solid leads to a reduction of the pore volume/porosity. In the current case, these reaction rates are simple, but in general any conceivable reaction can be defined in the model. If we assume that the densities for external and internal liquid, and the reacted solid are the same ($\rho_{\mathrm{l_e}} = \rho_{\mathrm{l_i}} = \rho_{\mathrm{s_r}}$), the changes of the independent properties of a particle due to chemical reaction are obtained by

$$\frac{\mathrm{d}s_{\mathrm{o}}}{\mathrm{d}t} = 0, \tag{23}$$

$$\frac{\mathrm{d}s_{\mathrm{r}}}{\mathrm{d}t} = r_{\mathrm{reac,e}} + r_{\mathrm{reac,i}}, \tag{24}$$

$$\frac{\mathrm{d}l_{\mathrm{e}}}{\mathrm{d}t} = -r_{\mathrm{reac,e}}, \tag{25}$$

$$\frac{\mathrm{d}p}{\mathrm{d}t} = \frac{\mathrm{d}l_{\mathrm{i}}}{\mathrm{d}t} = -r_{\mathrm{reac,i}}. \tag{26}$$

2.2.5 Penetration

A liquid droplet which coalesces with a "real" particle will increase the amount of external liquid of the new particle. If this particle is porous, external liquid will probably penetrate into the pores. To deal with this process, the following equation for the penetration rate r_{pen} is proposed:

$$r_{\mathrm{pen}} = k_{\mathrm{pen}}\, l_{\mathrm{e}}\, \left(p - l_{\mathrm{i}}\right). \tag{27}$$

The penetration rate r_{pen} is proportional to the amount of external liquid l_{e} and depends also on the remaining empty pore volume $(p - l_{\mathrm{i}})$. The rate law is rather simple for the moment, but as before there are no restrictions on the incorporation of a more complicated law in the future. The changes of the independent properties of a granule due to

penetration are given by

$$\frac{\mathrm{d}s_\mathrm{o}}{\mathrm{d}t} = 0, \quad \frac{\mathrm{d}s_\mathrm{r}}{\mathrm{d}t} = 0, \tag{28}$$

$$\frac{\mathrm{d}l_\mathrm{e}}{\mathrm{d}t} = -r_\mathrm{pen}, \tag{29}$$

$$\frac{\mathrm{d}l_\mathrm{i}}{\mathrm{d}t} = r_\mathrm{pen}, \tag{30}$$

$$\frac{\mathrm{d}p}{\mathrm{d}t} = 0. \tag{31}$$

2.2.6 Breakage

While breakage has been identified to be a significant process in high shear and drum granulation [2], the modelling of breakage in granulation processes is not so advanced. For instance, experiments in order to investigate the breakage behaviour of single wet granules have been performed [5], but a model was not derived. In the current work, a general event-driven description of wet granule breakage is used to account for operating conditions, the constituent material properties, and the granule properties.

For the characterisation of a breakage process, the likelihood of breakage of any particle and the properties distribution (e. g. size distribution) of the newly formed particles have to be known. The likelihood of breakage is described by the breakage frequency $g(x)$. The breakage frequency is seen to be proportional to the particle volume v, for parent particles larger than a minimum size $v_\mathrm{parent,min}$. In [11] it is mentioned that granules with high porosity are weak. This means that the probability of their breaking should be higher than for less porous particles. The granules are covered by external liquid on the outer surface. It is expected that a particle with a considerable amount of external liquid is weaker than a particle without it. These considerations lead to the breakage frequency of a particle with the properties x and is calculated by the following equation:

$$g(x) = \begin{cases} k_\mathrm{att}\ (\varepsilon + \chi)\ v & \text{, if} \quad v \geq v_\mathrm{parent,min} \\ 0 & \text{, otherwise} \end{cases}, \tag{32}$$

$$\text{with} \quad \varepsilon = \frac{p}{v}\ , \quad \chi = \frac{l_\mathrm{e}}{v}.$$

We assume that the breakage of wet granules has binary character. This means that breakage of a particle leads to one daughter particle and the remaining parent particle. The probability density f_att of the volume of the abraded daughter particle is modelled with a beta distribution.

$$f_\mathrm{att}(\Theta) = \frac{1}{B(a,b)}\,\Theta^{a-1}\,(1-\Theta)^{b-1} \quad \text{with} \quad B(a,b) = \int_0^1 \Theta^{a-1}\,(1-\Theta)^{b-1}\,\mathrm{d}\Theta \tag{33}$$

The parameter a and b determine the skewness of the function. The volume of a fragment will be in the range $[v_\mathrm{frag,min}; v_\mathrm{frag,max}]$ and depends on the material properties and loading conditions. For the use of the beta distribution in the described model, the variable Θ is defined as followed:

$$\Theta = \frac{v_\mathrm{frag} - v_\mathrm{frag,min}}{v_\mathrm{frag,max} - v_\mathrm{frag,min}}, \tag{34}$$

where v_{frag} denotes the total volume of the new fragment. The minimum fragment size $v_{\mathrm{frag,min}}$ is a constant value for all parent particles, whereas the maximum fragment size $v_{\mathrm{frag,max}}$ is dependent upon the total volume of the parent particle according to

$$v_{\mathrm{frag,max}} = \nu_{\mathrm{max}}\, v_{\mathrm{parent}} \qquad (\nu_{\mathrm{max}} \leq 0.5). \tag{35}$$

As the maximum fragment size can not be smaller than the minimum fragment size, a further constraint has to be introduced, namely that

$$v_{\mathrm{frag,max}} \geq \nu_{\mathrm{min,max}}\, v_{\mathrm{frag,min}} \qquad (\nu_{\mathrm{min,max}} \in [1; \infty)). \tag{36}$$

The combination of eqs. (35) and (36) gives a definition of the smallest parent particle,

$$v_{\mathrm{parent,min}} = \frac{\nu_{\mathrm{min,max}}}{\nu_{\mathrm{max}}}\, v_{\mathrm{frag,min}}. \tag{37}$$

Although the total size of the daughter particle is now defined, the composition is still unknown. We keep the model simple and assume that the composition of the new particles is the same as that of the parent particle, unless the parent particle is not porous. In this case, the daughter particle consists of external liquid only.

2.3 Numerical solution

The above model can be written in the form of a multidimensional population balance equation with five independent variables. Due to the complexity it is necessary to solve these equations numerically. In principal any methods can be chosen, although finite element approaches/sectional methods have the drawback that the computational effort required to obtain a solution grows exponentially with the number of independent variables [14]. We decided to use a Monte Carlo method to solve the model and chose a direct simulation algorithm (DSMC), because the particles of the real system can be represented by a smaller number of computational particles [6, 24, 15]. The structure of our coagulation kernel allows us to make use of fictitious jumps [3], which further increases the efficiency of the algorithm. Further reduction of the computational effort can be achieved by the application of the Linear Process Deferment Algorithm [19]. As our model also includes linear processes such as chemical reaction, we use this algorithm to obtain solutions of the model.

3 Discussion of simulation results and experimental validation

In this section we show the applicability of our model with a comparison between experimental and simulation results, and perform parameter studies for the reaction rate and the droplet size. Given that the multidimensional model is significantly dependent on binder distribution within the granular ensemble, an experiment was chosen to measure both granule size and granule binder concentration. The size was measured directly by

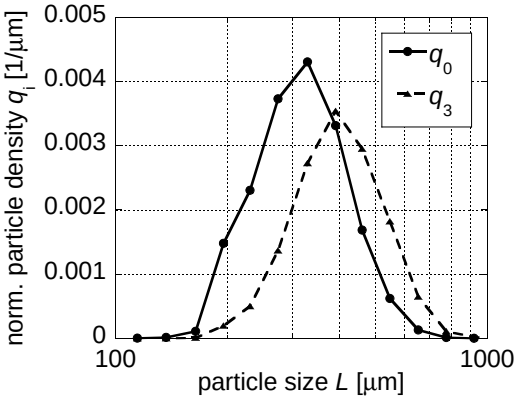

Figure 1: *Normalised number (q_0) and volume density function (q_3) of the dry feedstock*

automated image analysis. An optical tracer was added to the binder and granule colour was used as a proxy measure of binder concentration. A reactive binder-powder system is used to investigate the reaction sub-model.

To examine the model's capability to describe binder distribution as an event-driven process, we used a binder droplet size that is an order of magnitude larger than the particulate solids. Thus, the full dispersion of binder relies on events leading to contact-spreading. The reliance on contact spreading is common in many industrial applications, especially for fine-powder granulation.

3.1 Comparison between experiment and simulation

The experimental system used anhydrous sodium carbonate particles (FMC Soda Ash Grade 260) and a 25 wt% PEG-4000 aqueous solution binder in a bench scale high shear mixer. To track the distribution of the binder, a small amount (2 wt%) of an ultramarine blue pigment was added to the binder solution. Semi-automated optical measurements (Solids Sizer, JM Canty, Lockport, NY) were performed at different time intervals throughout the process, collecting both size and colour data of ~ 10000 particles per interval. The relative amount of reflected blue light was measured, averaged on a per-particle basis. The relative blue level (%B) is a proxy indicator of the binder amount/coating level, because the binder contains blue pigment. The light reflection was measured as an RGB composition so that a non-coated/white particle reflects red, green, and blue light equally.

The anhydrous powder reacts with water in the binder to form a monohydrate phase, effectively converting one mole of liquid water to a solid monohydrate ($\mathrm{Na_2CO_3 + H_2O \rightarrow Na_2CO_3 \cdot H_2O}$). This reaction occurs at the interface between the solid and liquid reactants, i. e., at the surface of the carbonate particles when contacted by the aqueous binder. Thus, the rate of the reaction is significant as it directly effects the liquid layer thickness on the particles, and therefore the value of the critical Stokes number.

The experiment started with a dry feedstock of non-porous particles. The normalised number and volume density functions of the feedstock are shown in fig. 1. The granu-

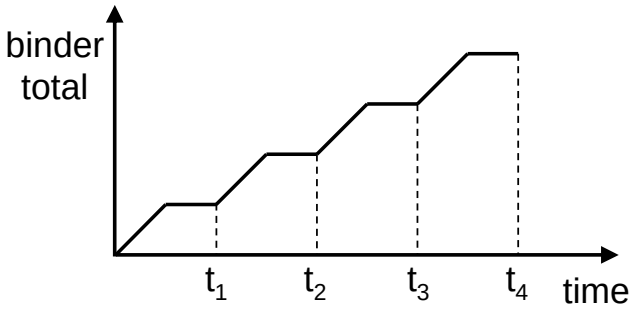

Figure 2: *Profile of the total binder amount*

Table 2: *Binder amounts after the different stages*

stage	binder amount [wt%]
t_0	0
t_1	5
t_2	10
t_3	15
t_4	20

lation was performed in four equally timed stages. During the first two-thirds of each stage binder was added dropwise from a syringe, whereas during the rest of the stage no binder addition took place. The droplet size from the syringe was $\sim 1\,\mathrm{mm}$ in diameter. The process profile of the total binder amount added over four intervals as shown in fig. 2 was chosen to allow for intermittent sampling of the material. After each interval, the mixer was switched off and a sample was taken to measure the size and the binder amount/coating level of the particles. Table 2 summarises the binder amounts which are obtained after every stage. The results of the particle measurements after each stage are shown in fig. 3. The particle distributions are plotted as a function of the particle size and the coating level in terms of the relative intensity of blue light reflected (%B). The increase in blue colour at small binder amounts is evidence of coating; however, a significant onset in granular size growth does not occur until $\sim 10\,\mathrm{wt}\%$ binder is added.

Simulations with the same conditions and profiles were performed. Many rate constants and material properties are contained in the model. Some of these parameters are known or can be reasonably approximated; others (e. g. , breakage functions) require empirical adjustment and/or further investigation. The predicted evolution of the binder dispersion and granule growth distributions are shown in fig. 4. We refer to this simulation in subsequent considerations as the 'reference case'. The simulation results also allow the volume mean size and standard deviation of this measure to be deduced. A comparison for both of these characteristics of the particle ensemble is made in fig. 5. From the previous figures it can be concluded that there is close agreement between the trends of the experiment and the simulation (reference case). The characteristic particle measures of the simulation are of the right order of magnitude follow similar trends. Although there is a remarkable dif-

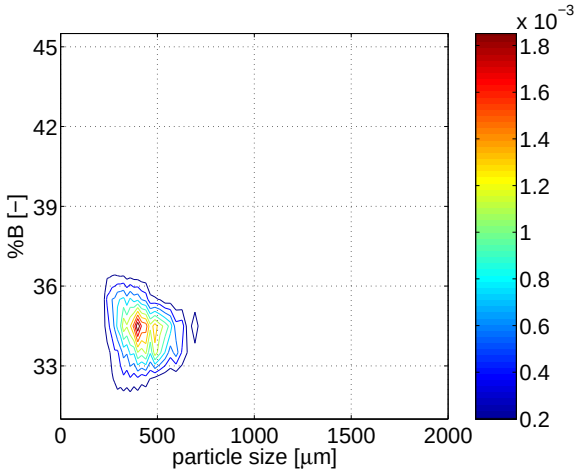

(a) At the start (t_0), 0 wt% binder amount (dry particles)

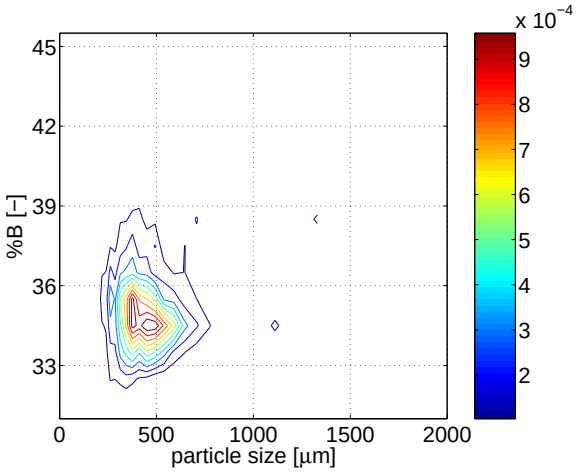

(b) At t_1, 5 wt% binder amount

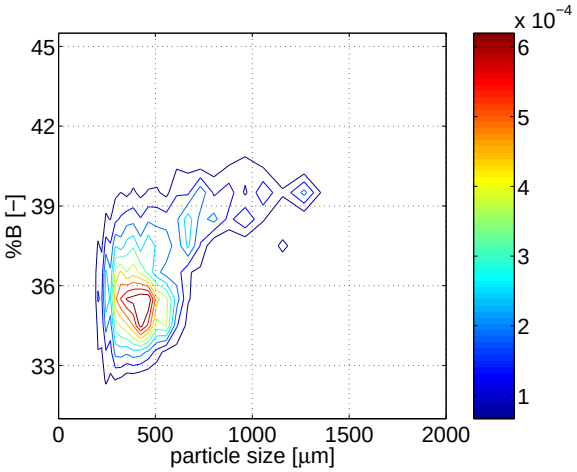

(c) At t_2, 10 wt% binder amount

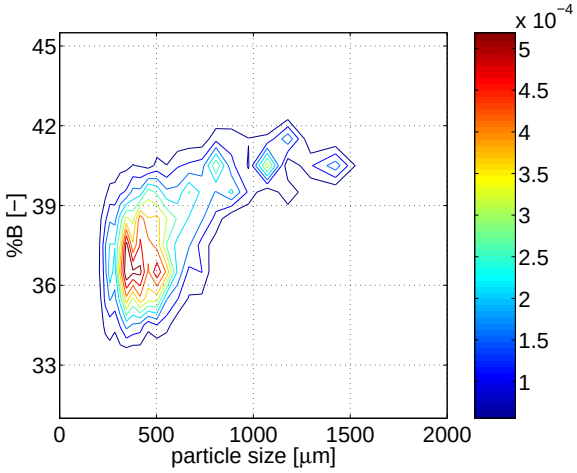

(d) At t_3, 15 wt% binder amount

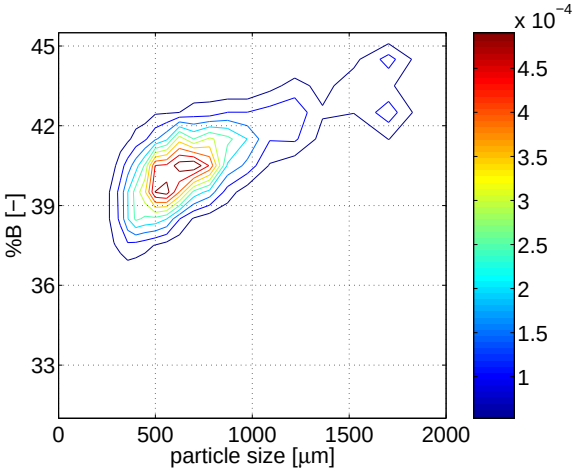

(e) At t_4, 20 wt% binder amount

Figure 3: *Normalised volume-binder amount-densities of the experiments (t_0–t_4)*

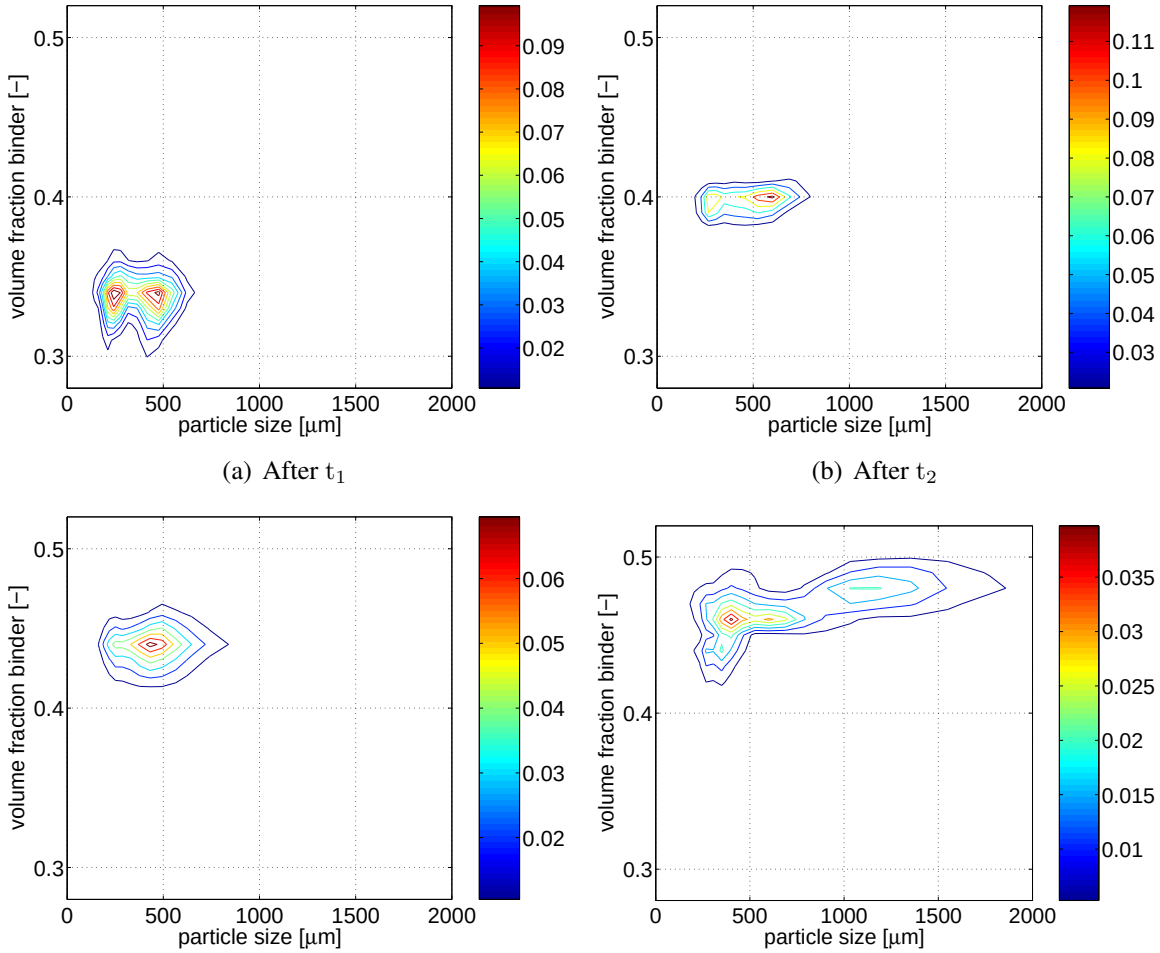

(a) After t_1

(b) After t_2

(c) After t_3

(d) After t_4

Figure 4: *Normalised particle distributions of the reference case (t_1–t_4)*

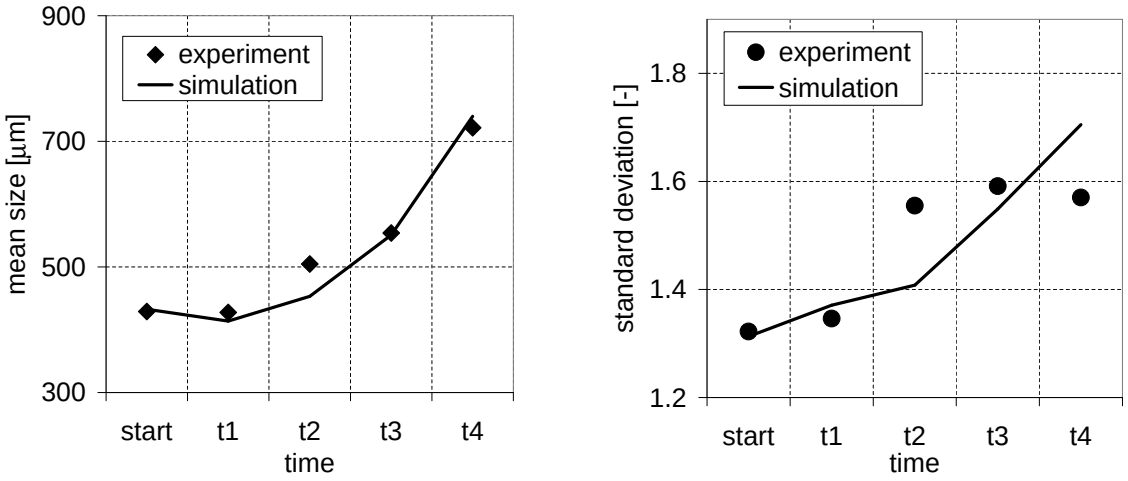

(a) Volume mean size

(b) Standard deviation of the volume mean size

Figure 5: *Comparison between experiment and simulation (reference case) for the geometric volume mean size and the standard deviation thereof*

ference between experiment and simulation for the t_2 stage, especially for the standard deviation, the model gives a promising qualitative prediction of the process evolution. An hypothesis for the divergence at the t_2 stage is that the model assumes perfect bulk mixing in the vessel while the experiment may have suffered localised heterogeneity in flow fields, thus increasing the standard deviation of the binder distribution due to contact spreading.

3.2 Parameter variations

A new feature of the model is the incorporation of chemical reactions in a single granule. As in the present case this can be the solidification of binder. If the reaction rate varies (e. g. due to different process conditions like temperature), the outcome of the granulation process is different from the reference case. The reaction rate constants were decreased and increased by an order of magnitude, so that the evolutions of the volume mean size and the standard deviation as in fig. 6 can be obtained. A reduction of the reaction rate leads to the formation of bigger final granules, whereas a higher reaction rate inhibits the size enlargement process. Not only the volume mean size of the particle ensemble increases with a reduced reaction rate, also the spread of the particle size rises. A possible explanation for this finding might be that a granule with the same composition can undergo more successful collisions in the first case, as more external liquid is present on the external surface. Furthermore, this particle is softer (lower coefficient of restitution), because the amount of internal liquid is higher for a lower reaction rate. These findings are supported by a plot of the mean critical STOKES number St^*_m versus time (fig. 7(a)). The mean critical Stokes number is calculated as particle volume weighted measure. This avoids the overestimation of small particles in an ensemble with large particles. Fig. 7 suggests that as lower the reaction rate is, as higher is the mean critical STOKES number St^*_m, i. e. the likelihood for the formation of granules increases. A negative mean critical

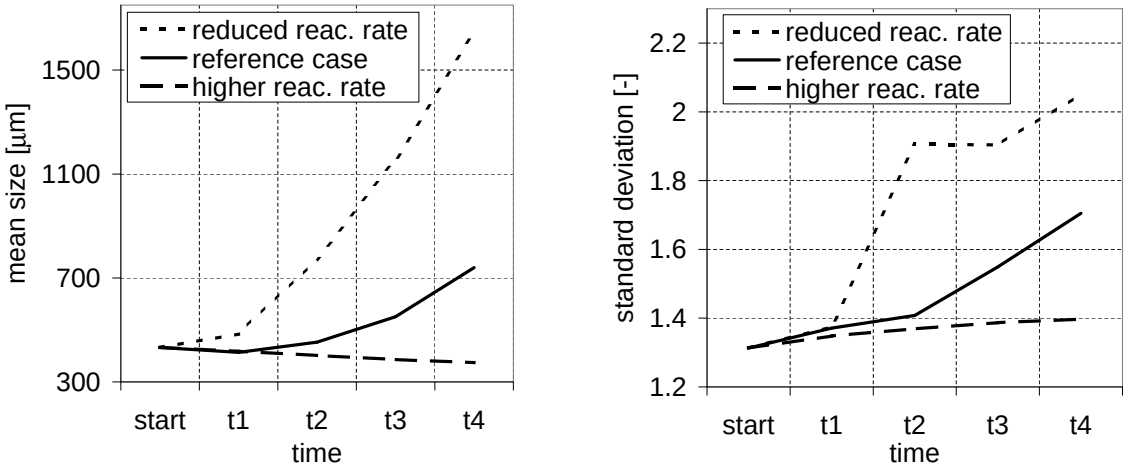

(a) Volume mean size (b) Standard deviation

Figure 6: *Geometric volume mean size and standard deviation in dependence of the reaction rate*

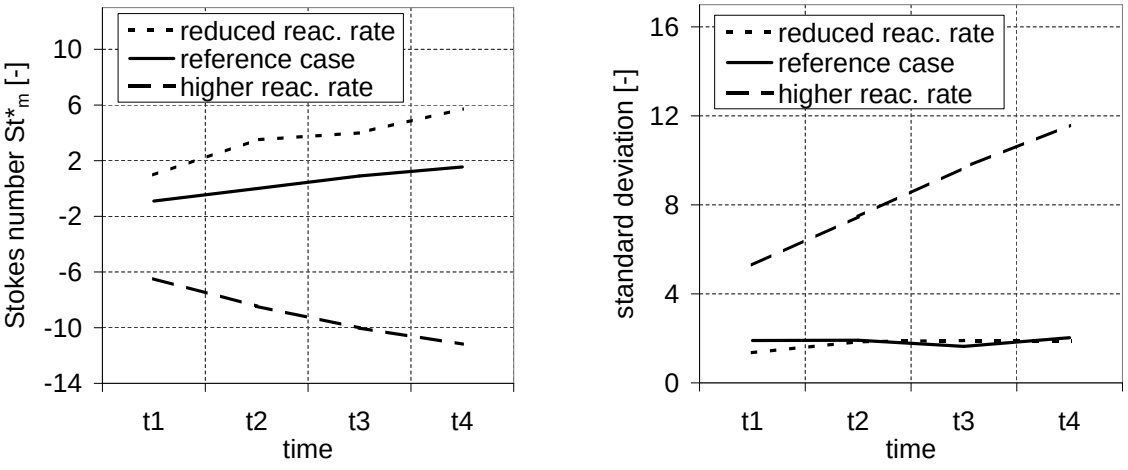

(a) Mean critical Stokes number (b) Standard deviation

Figure 7: *Mean critical Stokes number* $\mathrm{St}_{\mathrm{m}}^{*}$ *and standard deviation thereof in dependence of the reaction rate*

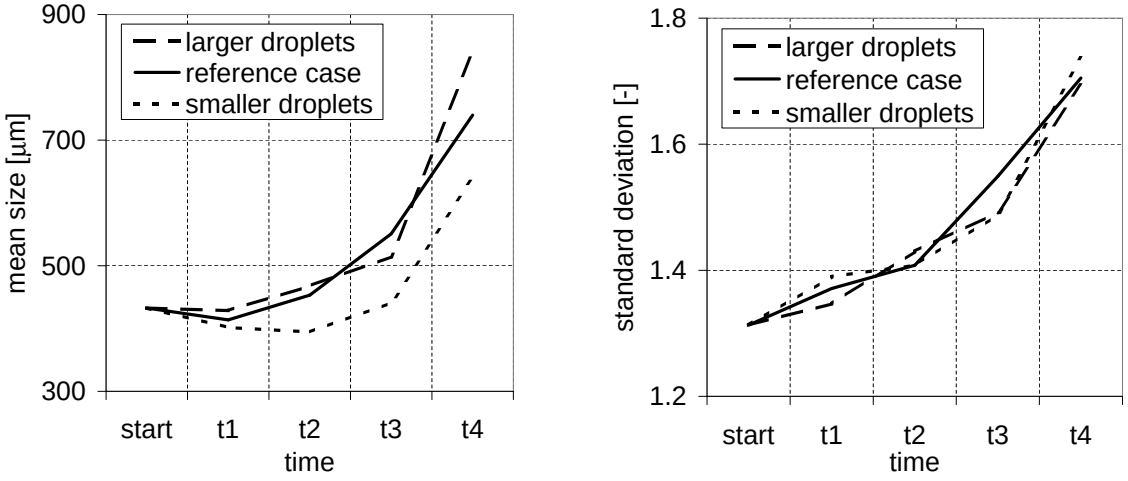

(a) Volume mean size

(b) Standard deviation

Figure 8: *Geometric volume mean size and standard deviation thereof with a variation of the droplet size*

STOKES number $\mathrm{St}_{\mathrm{m}}^{*}$ means, that the majority of the particles has not sufficient enough binder on the external surface in order to allow damping after a collision with a particle without binder. While the reduction of the reaction rate constant has hardly any influence on the standard deviation of the critical Stokes number, there is a remarkable increase in the standard deviation at higher reaction rate (fig. 7(b)). The increase in the critical Stokes standard deviation at high reaction rates reflects the increased variation of the liquid phase binder layer thickness due to the competition between contact spreading and the solidification reaction.

Indeed, the dispersion of the binder is of critical importance in the reactive granulation process. One may ask what happens, if the droplet size is changed, i. e. another nozzle configuration is used for the process. If the droplet size is changed by an order of magnitude with respect to the reference case, the results shown in fig. 8 are obtained. The addition of smaller droplets leads, on average, to smaller product sizes. A possible explanation for this finding might be that finer dispersion of the binder leads to a greater total interface between liquid and original solid, so that the binder solidifies faster and there is less coalescence of the particles. This is also shown by the mean critical STOKES number $\mathrm{St}_{\mathrm{m}}^{*}$ plotted in figure 9(a). The combined effects of a higher binder solidification rate and smaller binder droplets is consistent with particle coating practise, where a uniform film is desired and agglomeration is suppressed.

4 Conclusions

This paper presents a stochastic population balance model for binder granulation. The model is capable of using discrete event-driven sub-models to describe individual micro-scale transformations within an overall process model framework. As such, the stochastic method framework serves as an integrator of transformations within the overall process.

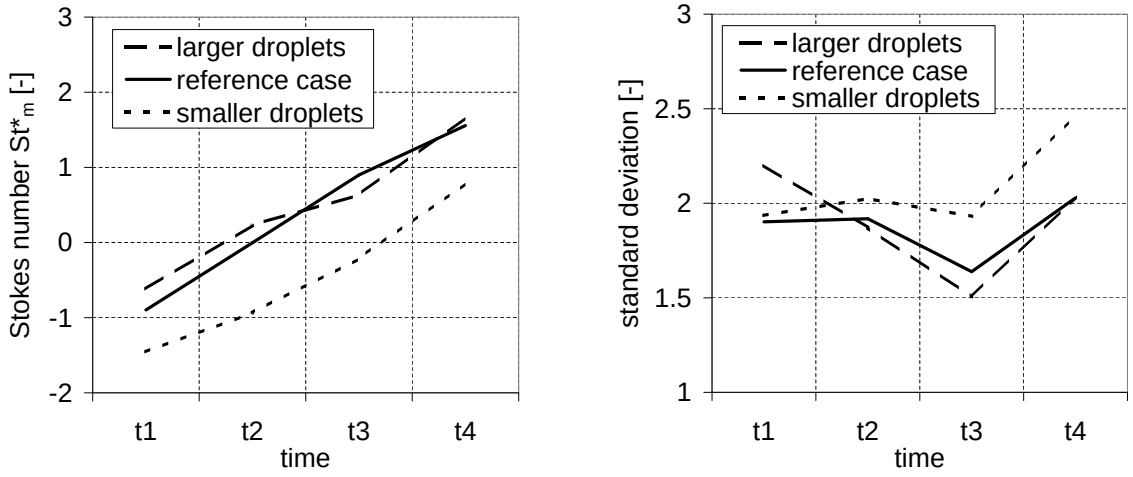

(a) Mean critical Stokes number

(b) Standard deviation

Figure 9: *Mean critical Stokes number* $\mathrm{St}_{\mathrm{m}}^{*}$ *and standard deviation in dependence of the droplet size*

A significant outcome of the current work is the incorporation of an explicit binder reaction rate (transformation from liquid to solid phase) within the granulation process as well as the combined dispersion of binder by both droplet atomization and contact-spreading mechanisms. The particles are described by five independent state properties to describe composition and structure, enabling consideration of multiple concurrent transformations including binder atomization, dispersion, coagulation, binder-substrate reactions, compaction and breakage. First comparisons between experiment and simulation show a promising agreement, and further in-silico case studies show significant effect of binder-related transformations on the product distributions, both in size and composition. Overall, the potential to bridge the micro and unit-operation scales using the stochastic modelling approach is a very promising development, and the authors foresee expanding opportunities to use this approach with more complex transformational models.

Acknowledgements

Andreas Braumann would like to thank Procter and Gamble, and the University of Cambridge for funding. Markus Kraft thanks Churchill College for financial support.

References

[1] A. A. Adetayo, J. D. Litster, S. E. Pratsinis, and B. J. Ennis. Population balance modelling of drum granulation of material with wide size distribution. Powder Technology, 82:37 – 49, 1995.

[2] I. T. Cameron, F.Y. Wang, C. D. Immanuel, and F. Stepanek. Process systems modelling and applications in granulation: A review. Chemical Engineering Science, 60:3723 – 3750, 2005.

[3] A. Eibeck and W. Wagner. An efficient stochastic algorithm for studying coagulation dynamics and gelation phenomena. SIAM Journal on Scientific Computing, 22(3):802 – 821, 2000.

[4] B. J. Ennis, G. Tardos, and R. Pfeffer. A microlevel-based characterization of granulation phenomena. Powder Technology, 65:257 – 272, 1991.

[5] J. Fu, G. K. Reynolds, M. J. Adams, M. J. Hounslow, and A. D. Salman. An experimental study of the impact breakage of wet granules. Chemical Engineering Science, 60:4005 – 4018, 2005.

[6] D. T. Gillespie. An exact method for numerically simulating the stochastic coalescence process in a cloud. Journal of the Atmospheric Sciences, 32(10):1977 – 1989, 1975.

[7] M. Goodson, M. Kraft, S. Forrest, and J. Bridgwater. A multi-dimensional population balance model for agglomeration. In PARTEC 2004 - International Congress for Particle Technology, 2004.

[8] K. P. Hapgood. Nucleation and binder dispersion in wet granulation. PhD thesis, University of Queensland, 2000.

[9] S. M. Iveson and J. D. Litster. Fundamental studies of granule consolidation, part 2: Quantifiying the effects of particle and binder properties. Powder Technology, 99:243 – 250, 1998.

[10] S. M. Iveson, J. D. Litster, and B. J. Ennis. Fundamental studies of granule consolidation, part 1: Effects of binder content and binder viscosity. Powder Technology, 88:15 – 20, 1996.

[11] S. M. Iveson, J. D. Litster, K. Hapgood, and B. J. Ennis. Nucleation, growth and breakage phenomena in agitated wet granulation processes: a review. Powder Technology, 117:3 – 39, 2001.

[12] W. Jander. Reaktionen im festen Zustande bei höheren Temperaturen, I. Mitteilung. Zeitschrift für anorganische und allgemeine Chemie, 163:1 – 30, 1927.

[13] P. C. Kapur and D. W. Fuerstenau. A coalescence model for granulation. Industrial and Engineering Chemistry: Process Design and Development, 8:56 – 62, 1969.

[14] M. Kraft. Modelling of particulate processes. KONA, 23:18 – 35, 2005.

[15] F. E. Kruis, A. Maisels, and H. Fissan. Direct simulation Monte Carlo method for particle coagulation and aggregation. AIChE Journal, 46(9):1735 – 1742, 2000.

[16] P. Mort and G. Tardos. Scale-up of agglomeration processes using transformations. KONA, 17:64 – 75, 1999.

[17] P. R. Mort, S. W. Capeci, and J. W. Holder. Control of agglomerate attributes in a continuous binder-agglomeration process. Powder Technology, 117:173 – 176, 2001.

[18] P. R. Mort and R. E. Riman. Hierarchically ordered particle mixtures by thermally-triggered granulation. KONA, 12:111 – 117, 1994.

[19] R. Patterson, J. Singh, M. Balthasar, M. Kraft, and J. R. Norris. The Linear Process Deferment Algorithm: A new technique for solving population balance equations. SIAM Journal on Scientific Computing, 28:303 – 320, 2006.

[20] G. K. Reynolds, J. S. Fu, Y. S. Cheong, M. J. Hounslow, and A. D. Salman. Breakage in granulation: A review. Chemical Engineering Science, 60:3969 – 3992, 2005.

[21] K. V. S. Sastry. Similarity size distribution of agglomerates during their growth by coalescence in granulation or green pelletization. Int. J. Min. Proc., 2:187 – 203, 1975.

[22] T. Schæfer and C. Mathiesen. Melt pelletization in a high shear mixer. IX. Effects of binder particle size. Int. J. Pharm., 139:139 – 148, 1996.

[23] T. Simmons, R. Turton, and P. Mort. An investigation into the effects of time and shear rate on the spreading of liquids in coating and granulation processes. In Fifth World Congress on Particle Technology, 2006.

[24] M. Smith and T. Matsoukas. Constant-number Monte Carlo simulation of population balances. Chemical Engineering Science, 53:1777 – 1786, 1998.

[25] G. I. Tardos, M. I. Khan, and P. R. Mort. Critical parameters and limiting conditions in binder granulation of fine powders. Powder Technology, 94:245 – 258, 1997.

[26] K. van den Dries, O. M. de Vegt, V. Girard, and H. Vromans. Granule breakage phenomena in a high shear mixer; influence of process and formulation variables and consequences on granule homogeneity. Powder Technology, 133:228–236, 2003.

[27] P. A. L. Wauters. Modelling and mechanisms of granulation. PhD thesis, Technische Universiteit Delft, 2001.